J. Korean Soc. Ind. Appl. Math. Vol.23, No.3, 157–178, 2019 http://doi.org/10.12941/jksiam.2019.23.157

SORET AND DUFOUR EFFECTS ON RADIATIVE HYDROMAGNETIC FLOW OF A CHEMICALLY REACTING FLUID OVER AN EXPONENTIALLY ACCELERATED INCLINED POROUS PLATE IN PRESENCE OF HEAT ABSORPTION AND VISCOUS DISSIPATION

M. VENKATESWARLU [1†], P. BHASKAR [2], AND D. VENKATA LAKSHMI [3]

[1]DEPARTMENT OF MATHEMATICS, V. R. SIDDHARTHA ENGINEERING COLLEGE, KRISHNA (DIST), A. P, INDIA, PIN: 520 007
Email address: mvsr2010@gmail.com

[2]DEPARTMENT OF MATHEMATICS, SHRI VENKATESHWARA UNIVERSITY, GAJRAULA, AMROHA (DIST), U. P, INDIA, PIN: 244 236
Email address: ponnabhaskar75@gmail.com

[3]DEPARTMENT OF MATHEMATICS, BAPATLA WOMEN'S ENGINEERING COLLEGE, BAPATLA, GUNTUR (DIST), A. P, INDIA, PIN: 522 102
Email address: himaja96@gmail.com

ABSTRACT. The present correspondence is conveyed on to consider the fascinating and novel characteristics of radiative hydromagnetic convective flow of a chemically reacting fluid over an exponentially accelerated inclined porous plate. Exact solutions for the fluid velocity, temperature and species concentration, under Boussinesq approximation, are obtained in closed form by the two term perturbation technique. The interesting parts of thermal dispersing outcomes are accounted in this correspondence. Graphical evaluation is appeared to depict the trademark direct of introduced parameters on non dimensional velocity, temperature and concentration profiles. Also, the numerical assortment for skin friction coefficient, Nusselt number and Sherwood number is examined through tables. The certification of current examination is confirmed by making an examination with past revelations available in composing, which sets a benchmark for utilization of computational approach.

1. INTRODUCTION

In recent years the problems of heat and mass transfer in presence of magnetic field through a porous medium have been attracted, the attention of several researchers because of their important applications in engineering and technology, such as compact heat exchangers, catalytic reactors, solar power collectors, paper production, rocket boosters, geothermal systems, heat insulation and film vaporization in combustion chambers. Li et al. [1] studied the compact heat

Received by the editors March 10 2019; Accepted September 4 2019; Published online September 25 2019.
2000 *Mathematics Subject Classification.* 78A40, 80A32, 80A20, 76DXX.
Key words and phrases. Soret effect, Dufour effect, Inclined plate, Heat absorption, Viscous dissipation.
† Corresponding author.

exchangers and future applications for a new generation of high temperature solar receivers. Hunt and Tien [2] presented the non-darcian flow, heat and mass transfer in catalytic packed-bed reactors. Leccese et al. [3] considered the convective and radiative wall heat transfer in liquid rocket thrust chambers. Khairnasov and Naumova [4] presented the heat pipes application to solar energy systems.

In several heat and mass transfer problems, the Dufour and Soret effects are neglected, on the basis that they are of a smaller order of magnitude than the effects described by Fourier's and Fick's laws. These effects are considered as second order phenomena and are significant in areas such as chemical reactors, drying processes, hydrology, geosciences, petrology etc. Some notable research studies on the topic are due to Postelnicu [5], Alam et al. [6], Afify [7], Venkateswarlu et al. [8], Olanrewaju and Makinde [9]. Makinde [10] studied the MHD mixed convection with soret and dufour effects past a vertical plate embedded in a porous medium. Venkateswarlu and Padma [11] presented the unsteady MHD free convective heat and mass transfer in a boundary layer flow past a vertical permeable plate with thermal radiation and chemical reaction. Venkateswarlu et al. [12] discussed the the influence of Hall current and heat source on MHD flow of a rotating fluid in a parallel porous plate channel. Venkateswarlu and Venkata Lakshmi [13] presented the Dufour and chemical reaction effects on unsteady MHD flow of a viscous fluid in a parallel porous plate channel under the influence of slip condition. Seth and Sarkar [14] considered the hydromagnetic natural convection flow with induced magnetic field and nth order chemical reaction of a heat absorbing fluid past an impulsively moving vertical plate with ramped temperature. Anjali Devi and Ganga [15] studied the effects of viscous and joules dissipation on MHD flow, heat and mass transfer past a stretching porous surface embedded in a porous medium.

It has been observed that combined heat and mass transfer flow with chemical reaction and thermal radiation is significant in many industrial and engineering applications, such as energy transfer in a wet cooling tower, evaporation at the surface of a water body, drying, and the flow in a desert cooler. Some of the relevant research studies are due to Hussanan et al. [16], Vedavathi et al. [17], Seth et al. [18], Venkatateswarlu et al. [19], Alam et al. [20], Tripathy et al. [21]. Venkateswarlu and Makinde [22] studied the unsteady MHD slip flow with radiative heat and mass transfer over an inclined plate embedded in a porous medium. Gnaneswara Reddy et al. [23] presented the effects of viscous dissipation and heat source on unsteady MHD flow over a stretching sheet. Venkateswarlu et al. [24] discussed the effects of chemical reaction and heat generation on MHD boundary layer flow of a moving vertical plate with suction and dissipation. Malapati and Dasari [25] presented the Soret and chemical reaction effects on the radiative MHD flow from an infinite vertical plate.

The objective of the present paper is to discuss the Soret and Dufour effects on radiative hydromagnetic flow of a chemically reacting fluid over an exponentially accelerated inclined porous plate with heat absorption and viscous dissipation. The behaviors of fluid velocity, temperature, concentration, skin-friction coefficient, Nusselt number and Sherwood number has been discussed in detail for variation of thermo physical parameters. The following strategy is pursued in the rest of the paper. Section two presents the formation of the problem. The analytical solutions are presented in section three. Results are discussed in section four and finally section five provides a conclusion of the paper.

2. Formation of the Problem

We consider an unsteady, radiative MHD natural convection flow of a viscous, incompressible, heat absorption and electrically conducting fluid over an exponentially accelerated inclined porous plate in the sight of observing consequences of Soret and Dufour effects. The physical model and coordinate system is shown in Fig. 1. The x - coordinate be taken in vertically upward direction along the plate with the angle of inclination α and y - coordinate is taken normal to the plate. In the energy equation, the dissipation of viscosity is considered. It is assumed that there exist a first order homogeneous chemical reaction with constant rate K_r^* between the fluid and diffusing species. The thin fluid is considered for the study is gray with absorbing/emitting radiation within a form of non- scattering medium. Initially at time $t \leq 0$, both the fluid and plate are at rest with uniform temperature T_∞ and uniform concentration C_∞. At time $t > 0$, plate starts with exponential velocity $u_0 \exp(iat)$ in x - direction. Under these assumptions, the boundary layer equations present the fluid flow, that is the momentum, energy and solutal concentration can be written as like Malapati and Dasari [25].

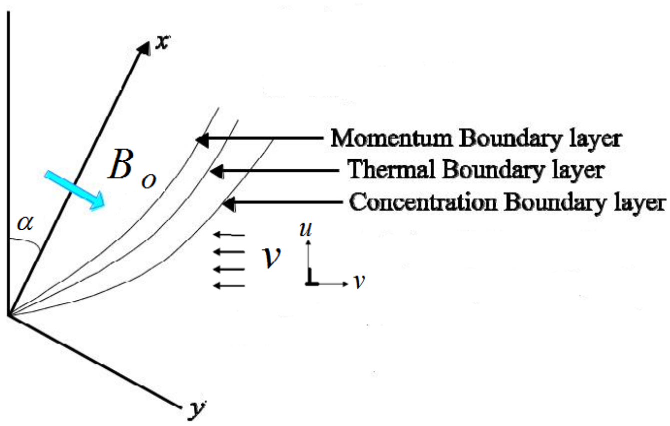

Figure 1: Schematic flow of the problem.

Continuity equation:

$$\frac{\partial v}{\partial y} = 0$$

Momentum equation:

$$\frac{\partial u}{\partial t} = \nu \frac{\partial^2 u}{\partial y^2} - \frac{\sigma_e B_0^2}{\rho} u + g\beta_T (T - T_\infty)\cos\alpha + g\beta_C (C - C_\infty)\cos\alpha - \frac{\nu}{K_1} u \tag{2.1}$$

$$0 = -\frac{1}{\rho}\frac{\partial p}{\partial y} - g\beta_T(T - T_\infty)\sin\alpha - g\beta_C(C - C_\infty)\sin\alpha \tag{2.2}$$

Energy equation:

$$\frac{\partial T}{\partial t} = \frac{K_T}{\rho c_p}\frac{\partial^2 T}{\partial y^2} + \frac{D_m K_T}{c_s c_p}\frac{\partial^2 C}{\partial y^2} - \frac{Q_0}{\rho c_p}(T - T_\infty) - \frac{1}{\rho c_p}\frac{\partial q_r}{\partial y} + \frac{\nu}{c_p}\left[\frac{\partial u}{\partial y}\right]^2 \tag{2.3}$$

Concentration equation:

$$\frac{\partial C}{\partial t} = D_m\frac{\partial^2 C}{\partial y^2} + \frac{D_m K_T}{T_m}\frac{\partial^2 T}{\partial y^2} - K_r^*(C - C_\infty) \tag{2.4}$$

where u - fluid velocity in x- direction, v - fluid velocity in y- direction, t - non dimensional time, ν - kinematic viscosity of the fluid, σ_e - fluid electrical conductivity , B_0 - magnetic induction, ρ - fluid density, g - acceleration due to gravity, β_T - coefficient of thermal expansion, T - fluid temperature, T_∞ - uniform temperature, α - angle of inclination, β_C - coefficient of concentration expansion, C - species concentration in the fluid, C_∞ - uniform concentration, K_1 - permeability of porous medium, p - fluid pressure, K_T - thermal diffusivity of the fluid, D_m - chemical molecular diffusivity, c_p - specific heat at constant pressure, c_s - concentration susceptibility, Q_0 - dimensional heat absorption parameter, q_r - radiating flux vector, T_m - mean fluid temperature and K_r^* - dimensional chemical reaction parameter respectively.

The pressure gradient term $-\frac{1}{\rho}\frac{\partial p}{\partial x}$ is absent in Eq. (2.1) because fluid flow is induced due to the movement of plate as well as buoyancy forces acting in x - direction. Equation (2.2) implies that fluid pressure p - varies in y - direction due to presence of buoyancy forces acting in y - direction. This means that change in fluid pressure from plate to the edge of the boundary layer varies due to change in thermal and solutal buoyancy forces.

We should in prior warn the reader that our model is not the same as that by Malapati and Dasari [25] in which the angle of inclination, Dufour effect and viscous dissipation were not taken into account. The corresponding initial and boundary conditions of the system of partial differential equations are given below

$$\left.\begin{array}{l} t \leq 0: \ u = 0, T = T_\infty, C = C_\infty \text{ for all } y \geq 0 \\ t > 0: u = u_o\exp(iat), T = T_w + \frac{(T-T_\infty)u_0^2}{(T_w-T_\infty)c_p}\exp(int), \\ C = C_w + \frac{(C-C_\infty)u_0^2}{(T_w-T_\infty)c_p}\exp(int) \text{ at } y = 0 \\ u \to 0, T \to T_\infty, C \to C_\infty \text{ as } y \to \infty \end{array}\right\}$$

where u_o - characteristic velocity, a - dimensional acceleration parameter, T_w - fluid temperature at the surface of the plate, C_w - species concentration at the surface of the plate and n - frequency of oscillation.

For an optically thick radiating fluid, we adopting the Rosseland approximation for radiating flux vector as (see, Magyari and Pantokratoras [26], Venkateswarlu et al. [27])

$$q_r = -\frac{4\sigma^*}{3a^*}\frac{\partial T^4}{\partial y} \tag{2.5}$$

Here a^* - mean absorption coefficient and σ^* - Stefan Boltzmann constant. We assume that the difference between fluid temperature T and free stream temperature T_∞ within the flow is sufficiently small such that T^4 may be expressed as a linear function of the temperature. This is accomplished by expanding T^4 in Taylor series about the free stream temperature T_∞ and neglecting the second and higher order terms, we have

$$T^4 = 4T_\infty^3 T - 3T_\infty^4 \tag{2.6}$$

Using Eqs. (2.5) and (2.6) in Eq. (2.3), we obtain

$$\frac{\partial T}{\partial t} = \frac{K_T}{\rho c_p}\left[1 + \frac{16\sigma^* T_\infty^3}{3a^* K_T}\right]\frac{\partial^2 T}{\partial y^2} + \frac{D_m K_T}{c_s c_p}\frac{\partial^2 C}{\partial y^2} - \frac{Q_0}{\rho c_p}(T - T_\infty) + \frac{\nu}{c_p}\left[\frac{\partial u}{\partial y}\right]^2 \tag{2.7}$$

We introduce the following non-dimensional variables

$$\eta = \frac{u_0}{\nu}y, \psi = \frac{u}{u_0}, \omega = \frac{\nu}{u_0^2}n, \tau = \frac{u_0^2}{\nu}t, b = \frac{\nu}{u_0^2}a, \theta = \frac{T - T_\infty}{T_w - T_\infty}, \phi = \frac{C - C_\infty}{C_w - C_\infty} \tag{2.8}$$

It may be noticed that characteristic velocity u_0 may be defined according to the non-dimensional process mentioned above as

$$u_0 = [g\beta_T \nu(T_w - T_\infty)]^{\frac{1}{3}} \tag{2.9}$$

By substituting Eqs. (2.8) and (2.9) into Eqs. (2.1), (2.4) and (2.7), we obtain the following non-dimensional partial differential equations

$$\frac{\partial \psi}{\partial \tau} = \frac{\partial^2 \psi}{\partial \eta^2} - \left[M + \frac{1}{K}\right]\psi + \theta cos\alpha + N\phi cos\alpha \tag{2.10}$$

$$\frac{\partial \theta}{\partial \tau} = \left[\frac{1+R}{Pr}\right]\frac{\partial^2 \theta}{\partial \eta^2} + Du\frac{\partial^2 \phi}{\partial \eta^2} - H\theta + Ec\left[\frac{\partial \psi}{\partial \eta}\right]^2 \tag{2.11}$$

$$\frac{\partial \phi}{\partial \tau} = \frac{1}{Sc}\frac{\partial^2 \phi}{\partial \eta^2} + Sr\frac{\partial^2 \theta}{\partial \eta^2} - Kr\phi \tag{2.12}$$

Here $N = \frac{\beta_C(C_w - C_\infty)}{\beta_T(T_w - T_\infty)}$ is the ratio of concentration buoyancy force and the thermal buoyancy force, $M = \frac{\sigma_e B_0^2 \nu}{\rho u_0^2}$ is the magnetic parameter, $K = \frac{K_1 u_0^2}{\nu^2}$ is the permeablity parameter, $Pr = \frac{\rho c_p \nu}{K_T}$ is the Prandtl number, $R = \frac{16a^* T_\infty^3}{3a^* K_T}$ is the radiation parameter, $Du = \frac{D_m K_T(C_w - C_\infty)}{c_s c_p \nu(T_w - T_\infty)}$ is the Dufour number, $H = \frac{Q_0 \nu}{\rho c_p u_0^2}$ is the heat absorption parameter, $Ec = \frac{u_0^2}{c_p(T_w - T_\infty)}$ is the Eckert number, $Sc = \frac{\nu}{D_m}$ is the Schmidt number, $Sr = \frac{D_m K_T(T_w - T_\infty)}{T_m \nu(C_w - C_\infty)}$ is the Soret number and $Kr = \frac{\nu}{u_0^2}k_r^*$ is the chemical reaction parameter respectively.

The corresponding initial and boundary conditions can be written as

$$\left.\begin{array}{l}\tau \leq 0 : \psi = 0,\ ,\theta = 0,\ \phi = 0 \text{ for all } \eta \geq 0 \\ \tau > 0 : \psi = \exp(ib\tau),\ \theta = 1 + Ec\exp(i\omega\tau),\ \phi = 1 + Ec\exp(i\omega\tau) \text{ at } \eta = 0 \\ \psi \to 0,\ \theta \to 0,\ \phi \to 0 \text{ as } \eta \to \infty\end{array}\right\}$$

It is now important to calculate physical quantities of primary interest, which are the local wall shear stress or skin friction coefficient, the local surface heat flux and the local surface mass flux. Given the velocity, temperature and concentration fields in the boundary layer, the shear stress τ_w , the heat flux q_w and mass flux j_w are obtained as

$$\tau_w = \mu \left[\frac{\partial u}{\partial y}\right]_{y=0} \tag{2.13}$$

$$q_w = -K_T \left[\frac{\partial T}{\partial y}\right]_{y=0} \tag{2.14}$$

$$j_w = -D_m \left[\frac{\partial C}{\partial y}\right]_{y=0} \tag{2.15}$$

In non-dimensional form the skin-friction coefficient Cf, heat transfer coefficient Nu and mass transfer coefficient Sh are defined as

$$Cf = \frac{\tau_w}{\rho u_0^2} \tag{2.16}$$

$$Nu = \frac{\nu}{u_o} \frac{q_w}{K_T(T_w - T_\infty)} \tag{2.17}$$

$$Sh = \frac{\nu}{u_o} \frac{j_w}{D_m(C_w - C_\infty)} \tag{2.18}$$

Using non-dimensional variables in Eq. (2.8) and Eqs. (2.13)-(2.15) into Eqs. (2.16)-(2.18), we obtain the physical parameters

$$Cf = \left[\frac{\partial \psi}{\partial \eta}\right]_{\eta=0}$$

$$Nu = -\left[\frac{\partial \theta}{\partial \eta}\right]_{\eta=0}$$

$$Sh = -\left[\frac{\partial \phi}{\partial \eta}\right]_{\eta=0}$$

3. Solution of the Problem

Equations (2.10)-(2.12) are coupled non-linear partial differential equations and these cannot be solved in closed form. So, we reduce these non-linear partial differential equations into a set of ordinary differential equations, which can be solved analytically. This can be done by assuming the trial solutions for the velocity, temperature and concentration of the fluid as (see, Siva Kumar et al. [28], Venkateswarlu et al. [29])

$$\psi(\eta, \tau) = \psi_0(\eta) + Ec\ \exp(i\omega\tau)\psi_1(\eta) + O(Ec^2) \tag{3.1}$$

$$\theta(\eta, \tau) = \theta_0(\eta) + Ec\ \ exp(i\omega\tau)\theta_1(\eta) + O(Ec^2) \tag{3.2}$$

$$\phi(\eta, \tau) = \phi_0(\eta) + Ec\ \exp(i\omega\tau)\phi_1(\eta) + O(Ec^2) \tag{3.3}$$

Substituting Eqs. (3.1)-(3.3) into Eqs. (2.10)-(2.12), then equating the harmonic and non-harmonic terms and neglecting the higher order terms of $0(Ec^2)$, we obtain

$$\psi_0^{''} - [M + \frac{1}{K}]\psi_0 = -[\theta_o cos\alpha + N\phi_o cos\alpha] \tag{3.4}$$

$$\psi_1^{''} - [M + \frac{1}{K} + i\omega]\psi_1 = -[\theta_1 cos\alpha + N\phi_1 cos\alpha] \tag{3.5}$$

$$\theta_0^{''} - \left[\frac{HPr}{1+R}\right]\theta_0 = -\left[\frac{PrDu}{1+R}\right]\phi_0^{''} \tag{3.6}$$

$$\theta_1^{''} - \left[\frac{Pr(H+i\omega)}{1+R}\right]\theta_1 = -\left[\frac{PrDu}{1+R}\right]\phi_1^{''} - \left[\frac{PrEc}{1+R}\right]\psi_o^{'2} \tag{3.7}$$

$$\phi_0^{''} - ScKr\phi_0 = -ScSr\theta_0^{''} \tag{3.8}$$

$$\phi_1^{''} - Sc[Kr + i\omega]\phi_1 = -ScSr\theta_1^{''} \tag{3.9}$$

where the prime denotes the ordinary differentiation with respect to η .

The corresponding initial and boundary conditions can be written as

$$\left.\begin{array}{l} \psi_0 = \exp(ib\tau), \psi_1 = 0, \theta_0 = 1, \theta_1 = 1, \phi_0 = 1, \phi_1 = 1 \text{ at } \eta = 0 \\ \psi_0 \to 0, \psi_1 \to 0, \theta_0 \to 0, \theta_1 \to 0, \phi_0 \to 0, \phi_1 \to 0 \text{ as } \eta \to \infty \end{array}\right\}$$

To slove the non linear differential equations (3.4)-(3.9), we assume that the Dufour number is small, so we can use $Du << 1$ as the perturbation parameter.

$$\psi_0(\eta, \tau) = \psi_{00}(\eta) + Du\ \psi_{01}(\eta) + O(Du^2) \tag{3.10}$$

$$\psi_1(\eta, \tau) = \psi_{10}(\eta) + Du\ \psi_{11}(\eta) + O(Du^2) \tag{3.11}$$

$$\theta_0(\eta, \tau) = \theta_{00}(\eta) + Du\ \theta_{01}(\eta) + O(Du^2) \tag{3.12}$$

$$\theta_1(\eta, \tau) = \theta_{10}(\eta) + Du\ \theta_{11}(\eta) + O(Du^2) \tag{3.13}$$

$$\phi_0(\eta, \tau) = \phi_{00}(\eta) + Du\ \phi_{01}(\eta) + O(Du^2) \tag{3.14}$$

$$\phi_1(\eta, \tau) = \phi_{10}(\eta) + Du\ \phi_{11}(\eta) + O(Du^2) \tag{3.15}$$

Substituting Eqs. (3.10)-(3.15) into Eqs. (3.4)-(3.9), then equating the harmonic and non-harmonic terms and neglecting the higher order terms of $0(Du^2)$, we obtain

$$\psi_{00}^{''} - [M + \frac{1}{K}]\psi_{00} = -[\theta_{00}\cos\alpha + N\phi_{00}\cos\alpha] \tag{3.16}$$

$$\psi_{01}^{''} - [M + \frac{1}{K}]\psi_{01} = -[\theta_{01}\cos\alpha + N\phi_{01}\cos\alpha] \tag{3.17}$$

$$\psi_{10}^{''} - [M + \frac{1}{K} + i\omega]\psi_{10} = -[\theta_{10}\cos\alpha + N\phi_{10}\cos\alpha] \tag{3.18}$$

$$\psi_{11}^{''} - [M + \frac{1}{K} + i\omega]\psi_{11} = -[\theta_{11}\cos\alpha + N\phi_{11}\cos\alpha] \tag{3.19}$$

$$\theta_{00}^{''} - \left[\frac{HPr}{1+R}\right]\theta_{00} = 0 \tag{3.20}$$

$$\theta_{01}^{''} - \left[\frac{HPr}{1+R}\right]\theta_{01} = -\left[\frac{Pr}{1+R}\right]\phi_{00}^{''} \tag{3.21}$$

$$\theta_{10}^{''} - \left[\frac{Pr(H+i\omega)}{1+R}\right]\theta_{10} = -\left[\frac{PrEc}{1+R}\right]\psi_{00}^{'2} \tag{3.22}$$

$$\theta_{11}^{''} - \left[\frac{Pr(H+i\omega)}{1+R}\right]\theta_{11} = -\left[\frac{Pr}{1+R}\right]\phi_{10}^{''} - \left[\frac{2PrEc}{1+R}\right]\psi_{00}^{'}\psi_{01}^{'} \tag{3.23}$$

$$\phi_{00}^{''} - ScKr\phi_{00} = -ScSr\theta_{00}^{''} \tag{3.24}$$

$$\phi_{01}^{''} - ScKr\phi_{01} = -ScSr\theta_{01}^{''} \tag{3.25}$$

$$\phi_{10}^{''} - Sc[Kr+i\omega]\phi_{10} = -ScSr\theta_{10}^{''} \tag{3.26}$$

$$\phi_{11}^{''} - Sc[Kr+i\omega]\phi_{11} = -ScSr\theta_{11}^{''} \tag{3.27}$$

The corresponding initial and boundary conditions can be written as

$$\left.\begin{array}{l} \psi_{00} = \exp(ib\tau), \psi_{01} = 0, \psi_{10} = 0, \psi_{11} = 0, \theta_{00} = 1, \theta_{01} = 0, \\ \theta_{10} = 1, \theta_{11} = 0, \phi_{00} = 1, \phi_{01} = 0, \phi_{10} = 1, \phi_{11} = 0 \text{ at } \eta = 0 \\ \psi_{00} \to 0, \psi_{01} \to 0, \psi_{10} \to 0, \psi_{11} \to 0, \theta_{00} \to 0, \theta_{01} \to 0, \\ \theta_{10} \to 0, \theta_{11} \to 0, \phi_{00} \to 0, \phi_{01} \to 0, \phi_{10} \to 0, \phi_{11} \to 0 \text{ as } \eta \to \infty \end{array}\right\} \tag{3.28}$$

The analytical solutions of Eqs. (3.16)-(3.27) with the boundary conditions in Eq. (3.28), are given by

$$\psi_{00} = A_6\exp(-m_1\eta) + A_7\exp(-m_2\eta) + A_8\exp(-m_3\eta) \tag{3.29}$$

$$\psi_{01} = A_{23}\exp(-m_1\eta) - A_{22}\exp(-m_2\eta) + A_{24}\exp(-m_3\eta) \tag{3.30}$$

$$\begin{aligned} \psi_{10} = A_{48}\exp(-m_6\eta) - A_{40}\exp(-m_4\eta) - A_{41}\exp(-m_5\eta) \\ +A_{42}\exp(-2m_3\eta) + A_{43}\exp(-2m_1)\eta + A_{44}\exp(-2m_2\eta) + \\ A_{45}\exp[-(m_1+m_3)]\eta + A_{46}\exp[-(m_1+m_2)]\eta + A_{47}\exp[-(m_2+m_3)]\eta \end{aligned} \tag{3.31}$$

$$\begin{aligned} \psi_{11} = A_{78}\exp(-m_6\eta) + A_{69}\exp(-m_4\eta) + A_{71}\exp(-m_5\eta) \\ +A_{72}\exp(-2m_1\eta) + A_{73}\exp(-2m_2)\eta + A_{74}\exp(-2m_3\eta) + \\ A_{75}\exp[-(m_1+m_2)]\eta + A_{76}\exp[-(m_2+m_3)]\eta + A_{77}\exp[-(m_1+m_3)]\eta \end{aligned} \tag{3.32}$$

$$\theta_{00} = \exp(-m_1)\eta \tag{3.33}$$

$$\theta_{01} = [A_9 + \eta A_{10}]\exp(-m_1)\eta - A_9\exp(-m_2)\eta \tag{3.34}$$

$$\begin{aligned} \theta_{10} = A_{31}\exp(-m_4\eta) - A_{26}\exp(-2m_1\eta) - A_{27}\exp(-2m_2)\eta \\ -A_{25}\exp(-2m_3\eta) - A_{29}\exp[-(m_1+m_2)]\eta - \\ A_{30}\exp[-(m_2+m_3)]\eta - A_{28}\exp[-(m_1+m_3)]\eta \end{aligned} \tag{3.35}$$

$$\begin{aligned} \theta_{11} = A_{57}\exp(-m_4\eta) - A_{49}\exp(-m_5\eta) - A_{50}\eta\exp(-m_4\eta) \\ -A_{51}\exp(-2m_1\eta) - A_{52}\exp(-2m_2)\eta - A_{53}\exp(-2m_3\eta) - \\ A_{54}\exp[-(m_1+m_2)]\eta - A_{55}\exp[-(m_2+m_3)]\eta - A_{56}\exp[-(m_1+m_3)]\eta \end{aligned} \tag{3.36}$$

$$\phi_{00} = A_4 \exp(-m_1\eta) + A_5 \exp(-m_2\eta) \tag{3.37}$$

$$\phi_{01} = A_{13} \exp(-m_1\eta) - [A_{13} + A_{11}\eta] \exp(-m_2\eta) \tag{3.38}$$

$$\begin{aligned}\phi_{10} = A_{39} \exp(-m_5\eta) - A_{32} \exp(-m_4\eta) + A_{33} \exp(-2m_3\eta) + \\ A_{34} \exp(-2m_1)\eta + A_{35} \exp(-2m_2\eta) + A_{36} \exp[-(m_1 + m_3)\eta] + \\ A_{37} \exp[-(m_1 + m_2)\eta] + A_{38} \exp[-(m_2 + m_3)\eta]\end{aligned} \tag{3.39}$$

$$\begin{aligned}\phi_{11} = [A_{67} - A_{60}\eta] \exp(-m_5\eta) + A_{59} \exp(-m_4\eta) + A_{61} \exp(-2m_1\eta) + \\ A_{62} \exp(-2m_2)\eta + A_{63} \exp(-2m_3\eta) + A_{64} \exp[-(m_1 + m_2)]\eta - \\ A_{65} \exp[-(m_2 + m_3)]\eta + A_{66} \exp[-(m_1 + m_3)]\eta\end{aligned} \tag{3.40}$$

By substituting Eqs. (3.29)-(3.40) into Eqs. (3.1)-(3.3), we obtained solutions for the fluid velocity, temperature and concentration and are presented in the following form

$$\psi(\eta, \tau) = [\psi_{00} + Du\, \psi_{01}] + Ec\ \exp(i\omega\tau)[\psi_{10} + Du\, \psi_{11}]$$
$$\theta(\eta, \tau) = [\theta_{00} + Du\, \theta_{01}] + Ec\ \exp(i\omega\tau)[\theta_{10} + Du\, \theta_{11}]$$
$$\phi(\eta, \tau) = [\phi_{00} + Du\, \phi_{01}] + Ec\ \exp(i\omega\tau)[\phi_{10} + Du\, \phi_{11}]$$

3.1 Skin friction: From the velocity field, the skin friction at the plate can be obtained, which is given in non dimensional form as

$$Cf = [\psi'_{00} + Du\, \psi'_{01}]_{\eta=0} + Ec\ \exp(i\omega\tau)[\psi'_{10} + Du\, \psi'_{11}]_{\eta=0}$$

3.2 Nusselt number : From temperature field, we obtained heat transfer coefficient which is given in non-dimensional form as

$$Nu = [\theta'_{00} + Du\, \theta'_{01}]_{\eta=0} + Ec\ \exp(i\omega\tau)[\theta'_{10} + Du\, \theta'_{11}]_{\eta=0}$$

3.3 Sherwood number : From concentration field, we obtained mass transfer coefficient which is given in non-dimensional form as

$$Sh = [\phi'_{00} + Du\, \phi'_{01}]_{\eta=0} + Ec\ \exp(i\omega\tau)[\phi'_{10} + Du\, \phi'_{11}]_{\eta=0}$$

4. Results And Discussion

The impacts of various governing non dimensional parameters are examined, namely the buoyancy parameter N, magnetic parameter M, permeability parameter K, angle of inclination α, Prandtl number Pr, radiation parameter R, Dufour number Du, heat absorption parameter H, Eckert number Ec, Schmidt number Sc, Soret number Sr, chemical reaction parameter Kr and acceleration parameter b in transit of flow field, fluid velocity ψ, temperature θ and solutal concentration ϕ are studied graphically in Figs 2-21. The comparative results are reported in Table 1. The results obtained reveals that our results and those of Malapati and Dasrari [25] are very good in agreement. The numerical values of skin friction coefficient Cf, heat transfer coefficient Nu and mass transfer coefficient Sh are presented in tables 2 and 3. In the present investigation following parameter values are adopted for computations: $\alpha = \frac{\pi}{4}$,

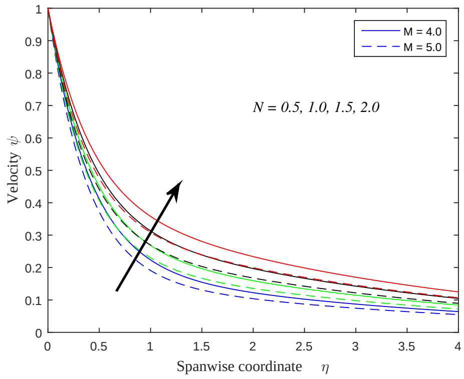

Figure 2: Influence of buoyancy parameter on velocity profiles.

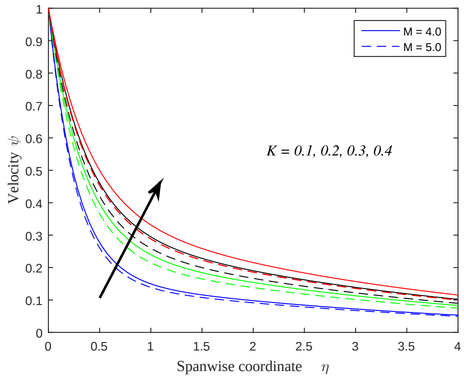

Figure 3: Influence of permeability parameter on velocity profiles.

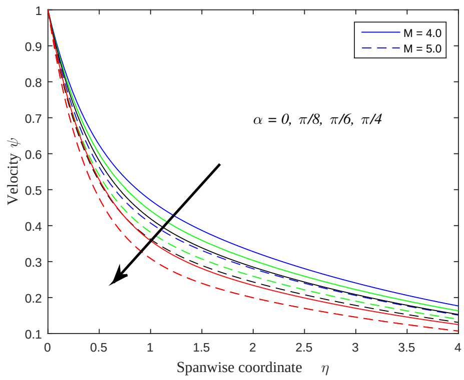

Figure 4: Influence of angle of inclination on velocity profiles.

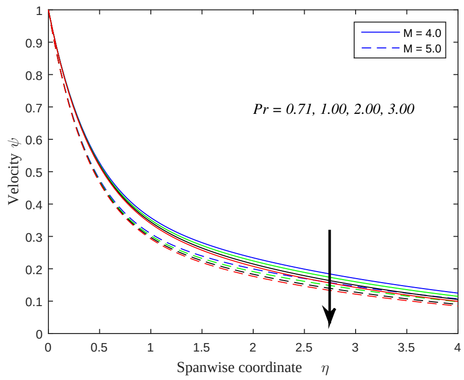

Figure 5: Influence of Prandtl number on velocity profiles.

$N = 2$, $M = 5$, $K = 0.5$, $Pr = 0.71$, $R = 1.0$, $Du = 0.1$, $H = 0.2$, $Ec = 0.2$, $Sc = 0.22$, $Sr = 1.0$, $Kr = 0.5$, $\tau = 1.0$, $b = 0.2$, $\omega = 1.0$. Hence all the graphs and tables correspond to these values unless specifically indicated on the appropriate graph or table.

It is noticed from the Figs. 2-13 that, the fluid velocity ψ corresponding to $M = 4$ is higher than the fluid velocity ψ corresponding to $M = 5$. Hence velocity ψ decreases on increasing the magnetic parameter M. It is noticed from the Figs. 14-18 that, the fluid temperature θ corresponding to air $(Pr = 0.71)$ is greater than the fluid temperature θ corresponding to electrolytic solution $(Pr = 1.00)$ with the parameters R, H, Ec and Kr whereas Du has a reverse

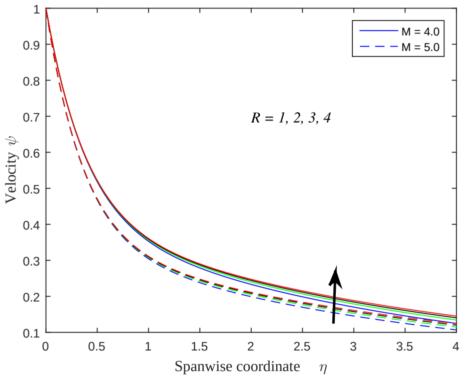

Figure 6: Influence of radiation parameter on velocity profiles.

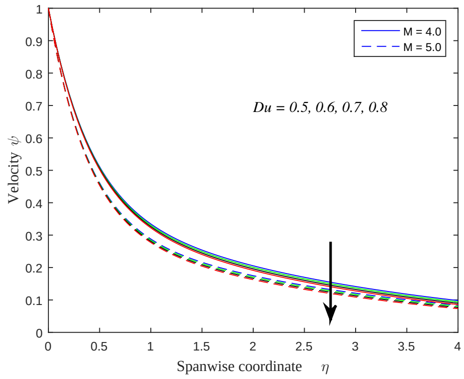

Figure 7: Influence of Dufour number on velocity profiles.

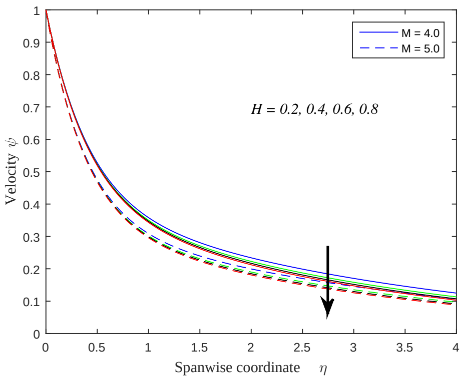

Figure 8: Influence of heat absorption parameter on velocity profiles.

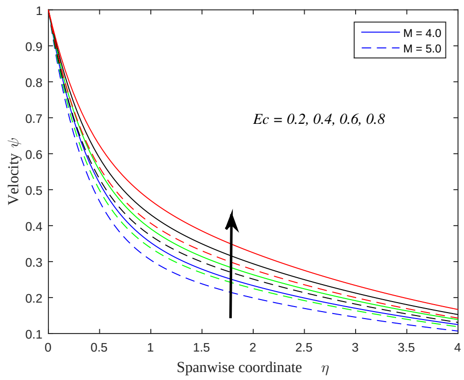

Figure 9: Influence of Eckert number on velocity profiles.

trend. It is observed from the Figs. 19-21 that, the species concentration ϕ corresponding to Hydrogen $(Sc = 0.22)$ is greater than the species concentration ϕ corresponding to Ammonia $(Sc = 0.78)$. Figure 2 depicts the influence of buoyancy parameter N on the fluid velocity ψ. The buoyancy parameter N defines the ratio of Solutal Grashof number Gm to thermal Grashof number Gr. It is evident from Fig. 2. velocity ψ increases on increasing the buoyancy parameter N. Figure 3 shows that an increase in the permeability parameter K results an increase in the velocity component ψ. For large porosity of the medium fluid acquires more space to flow as a consequence its velocity increases. It is observed from Fig. 4 that the velocity ψ is getting

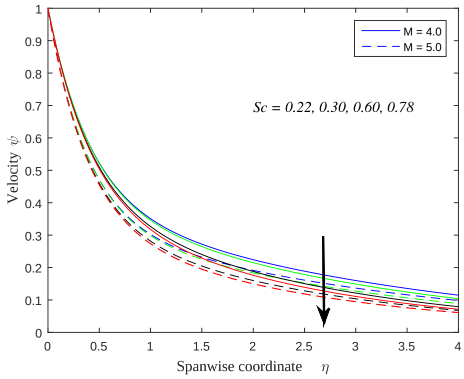

Figure 10: Influence of Schmidt number on velocity profiles.

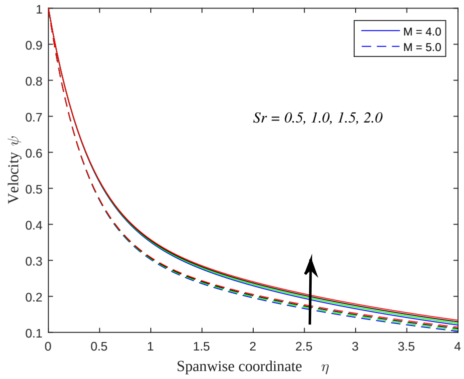

Figure 11: Influence of Soret number on velocity profiles.

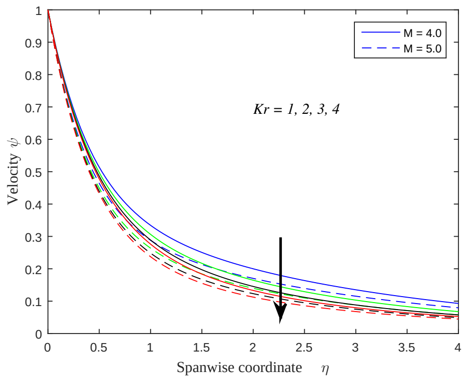

Figure 12: Influence of chemical reaction parameter on velocity profiles.

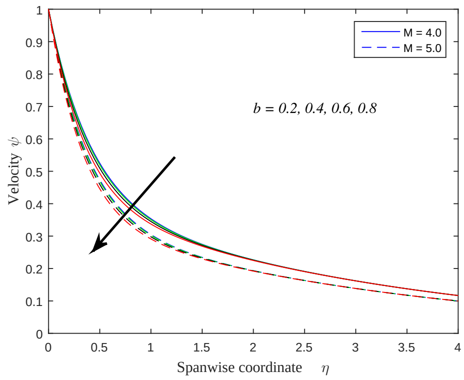

Figure 13: Influence of acceleration parameter on velocity profiles.

decelerated on increasing the angle of inclination α. This is because the effect of buoyancy force is getting reduced due to multiplication of the term $\cos\theta$ in the buoyancy force term. Since $\cos\theta$ assumes maximum value when $\theta = 0$ and it is getting reduced as θ increases. Due to this reason strength of buoyancy forces is getting reduced on increasing angle of inclination of the plate.

Figure 5 shows the fluid velocity ψ for different estimations of the Prandtl number Pr. Prandtl number characterizes the relative adequacy of the momentum transport by dispersion in the hydrodynamic boundary layer to the essentialness transported by thermal dispersion in

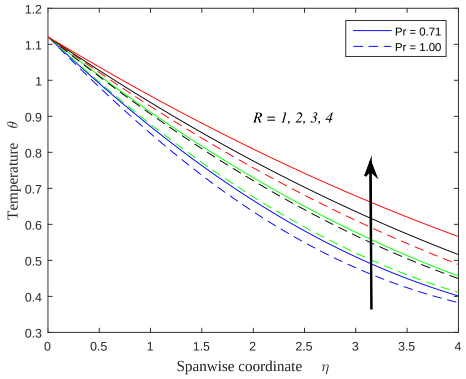

Figure 14: Influence of radiation parameter on temperature profiles.

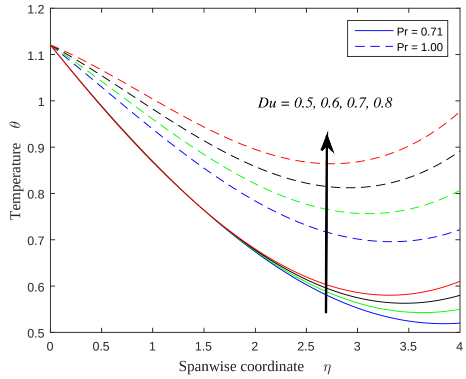

Figure 15: Influence of Dufour number on temperature profiles.

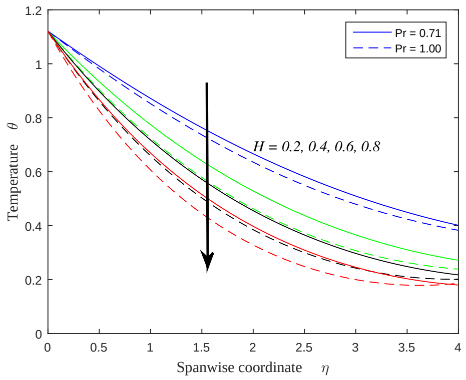

Figure 16: Influence of heat absorption parameter on temperature profiles.

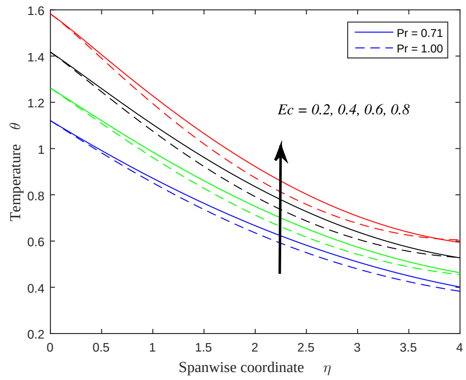

Figure 17: Influence of Eckert number on temperature profiles.

the thermal boundary layer. It is noticed that the velocity ψ decreases on increases the Prandtl number Pr. Figures 6 and 14 establishes that the fluid velocity ψ and temperature θ increases on increasing the radiation parameter R. This fact is justified because the fluid temperature θ increases on increase in R as observed from Fig. 14. This implies that the fluid temperature strengthen the thermal buoyancy force. Hence ψ is accelerated with an increase in R. Figures 7 and 15 describe the fluid velocity ψ and temperature θ for different values of Dufour number Du. The Dufour number signifies the contribution of the concentration gradient to the thermal energy flux in the flow. It is clear from Figs. 7 and 15 that the fluid velocity ψ decreases on

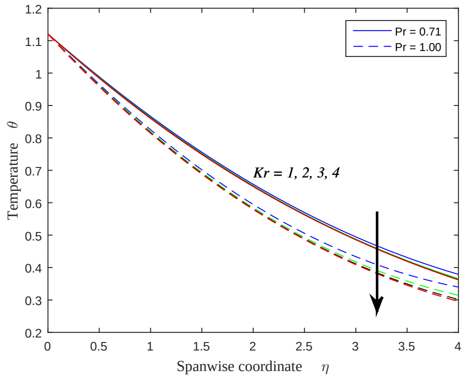

Figure 18: Influence of chemical reaction parameter on temperature profiles.

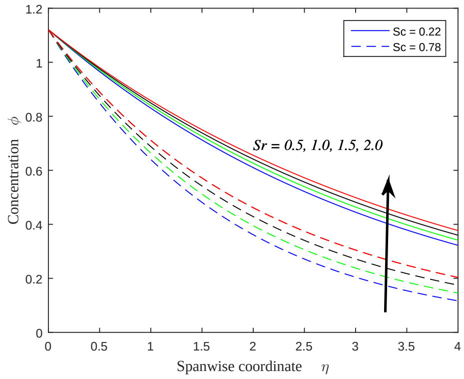

Figure 19: Influence of Soret number on concentration profiles.

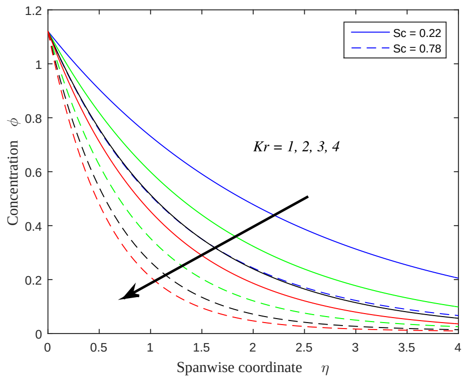

Figure 20: Influence of chemical reaction parameter on concentration profiles.

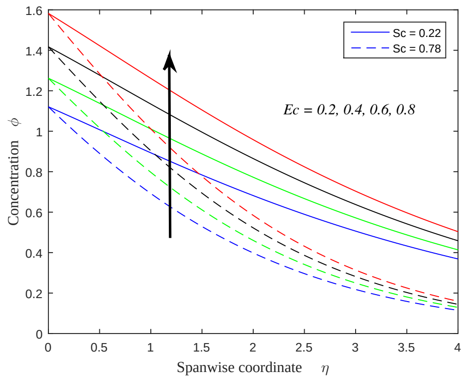

Figure 21: Influence of Eckert number on concentration profiles.

increasing the Dufour number Du where as the fluid temperature θ increases on increasing the Dufour number Du.

Figures 8 and 16 displays the impact of heat absorption parameter H on the fluid velocity ψ and temperature θ. It is evident that the fluid velocity ψ and temperature θ decreases on increasing the heat absorption parameter H. Figures 9, 17 and 21 shows the influence of Eckert number Ec on the fluid velocity ψ, temperature θ and concentration ϕ respectively. Eckert number defines the relationship between the kinematic energy in the flow and the enthalpy. It is observed that, the fluid velocity ψ, temperature θ and concentration ϕ experiences an enhancement on increasing the Eckert number Ec . This is due to the reason that Eckert number represents the conversion of kinematic energy into internal energy by work done against the viscous fluid stresses. The influence of fluid velocity ψ in presence of foreign species such as Hydrogen $(Sc = 0.22)$, Helium $(Sc = 0.30)$, Water vapour $(Sc = 0.60)$, Ammonia $(Sc = 0.78)$ is shown in Fig 10. Physically, Schmidt number signifies the relative strength of viscosity to chemical molecular diffusivity. Therefore the Schmidt number quantifies the relative effectiveness of momentum and mass transport by diffusion in the hydrodynamic and concentration boundary layers. This causes the concentration buoyancy effects to decrease the fluid velocity. It is observed that velocity ψ decreases on increasing Schmidt number Sc in Fig. 10.

Figures 11 and 19 demonstrate the influence of Soret number Sr on the fluid velocity ψ and concentration ϕ respectively. The Soret number defines the influence of the temperature gradient inducing significant mass diffusion effects. It is noticed that the fluid velocity ψ and concentration ϕ increases with an increase in Soret number Sr. Figures 12, 18 and 20 are plotted for different values of chemical reaction parameter Kr on the fluid velocity ψ, temperature θ and concentration ϕ respectively. It is observed that, the fluid velocity ψ, temperature θ and concentration ϕ decreases on increasing the chemical reaction parameter Kr. This implies that, chemical reaction tends to reduce the fluid velocity, temperature and species concentration. It is revealed from Fig. 13 that fluid velocity ψ decreases on increasing plate acceleration parameter b in the region near the plate and the effect of b is almost negligible in the region away from the plate.

The numerical values of skin friction coefficient Cf , heat transfer coefficient Nu and mass transfer coefficient Sh, obtained from the exact analytical solutions, are presented in tabular form in tables 1 and 2. It is clear that, the skin friction Cf increases on increasing the angle of inclination α, magnetic parameter M, Prandtl number Pr, heat absorption parameter H, chemical reaction parameter Kr and plate acceleration parameter b whereas it decreases on increasing the buoyancy parameter N, permeability parameter K, radiation parameter R, Dufour number Du, Eckert number Ec and Soret number Sr.

Heat transfer coefficient Nu decreases on increasing the buoyancy parameter N, permeability parameter K, Prandtl number Pr, Dufour number Du, heat absorption parameter H, Eckert number Ec, Soret number Sr,chemical reaction parameter Kr and plate acceleration parameter b whereas it increases on increasing the angle of inclination α, Magnetic parameter M and radiation parameter R.

Mass transfer coefficient Sh increases on increasing the buoyancy parameter N, permeability parameter K, Prandtl number Pr, heat absorption parameter H, Soret number Sr and plate acceleration parameter b whereas it decreases on increasing the angle of inclination α, Magnetic parameter M, radiation parameter R, Dufour number Du, Eckert number Ec and chemical reaction parameter Kr.

5. CONCLUSIONS

In the present investigation we have studied analytically Soret and Dufour effects on radiative MHD flow of a chemically reacting fluid over an exponentially accelerated inclined porous plate with heat absorption and viscous dissipation. From the present investigation the following conclusions can be drawn:

- Buoyancy parameter N and Eckert number Ec are tends to accelerate the fluid velocity ψ whereas they have a reverse effect on the skin friction coefficient Cf.
- Angle of inclination α and plate acceleration parameter b are tends to decelerate the fluid velocity ψ whereas they have a reverse effect on the skin friction coefficient Cf.
- The fluid velecity ψ and skin friction coefficien Cf decreases with increasing values of Dufour number Du.
- Dufour number Du and Eckert number Ec are tends to accelerate the fluid temperature θ whereas they have a reverse trend on the heat transfer coefficient Nu.
- Eckert number Ec accelerates the species concentration whereas it has a reverse trend on the mass transfer coefficient Sh.

ACKNOWLEDGMENTS

The authors wish to appreciate the constructive comments and suggestions of the anonymous reviewers.

Table 1: Comparision with the skin friction coefficient values (PST) of Malapati and Dasari [25] for different values of M, N and K when $\alpha = b = Du = R = 0$, $\epsilon = Ec = 0.001$, $Q = H = 5.0$, $Sr = 5.0$ and $\omega = 0.1$.

M	N	K	Ref [25]	Present
1.0	2.0	0.5	0.0122	0.0122
2.0	2.0	0.5	0.4940	0.4940
3.0	2.0	0.5	0.8798	0.8798
4.0	2.0	0.5	1.2058	1.2058
2.0	0.2	0.5	1.6174	1.6174
2.0	0.4	0.5	1.4926	1.4926
2.0	0.6	0.5	1.3678	1.3678
2.0	0.8	0.5	1.2429	1.2429
2.0	2.0	0.1	2.5756	2.5756
2.0	2.0	0.3	0.9940	0.9940
2.0	2.0	0.5	0.4940	0.4940
2.0	2.0	0.7	0.2340	0.2340

Table 2: Influence of N, M, K, α, b and R on Cf, Nu and Sh.

N	M	K	α	b	R	Cf	Nu	Sh
0.5	5.0	0.5	$\frac{\pi}{4}$	0.2	1.0	2.2356	-0.2837	-0.3236
1.0	5.0	0.5	$\frac{\pi}{4}$	0.2	1.0	2.1000	-0.2846	-0.3234
1.5	5.0	0.5	$\frac{\pi}{4}$	0.2	1.0	1.9645	-0.2854	-0.3232
2.0	5.0	0.5	$\frac{\pi}{4}$	0.2	1.0	1.8290	-0.2862	-0.3231
2.0	1.0	0.5	$\frac{\pi}{4}$	0.2	1.0	0.5529	-0.2904	-0.3224
2.0	2.0	0.5	$\frac{\pi}{4}$	0.2	1.0	0.9539	-0.2893	-0.3226
2.0	3.0	0.5	$\frac{\pi}{4}$	0.2	1.0	1.2868	-0.2882	-0.3227
2.0	4.0	0.5	$\frac{\pi}{4}$	0.2	1.0	1.5741	-0.2871	-0.3229
2.0	5.0	0.1	$\frac{\pi}{4}$	0.2	1.0	3.2981	-0.2803	-0.3242
2.0	5.0	0.2	$\frac{\pi}{4}$	0.2	1.0	2.4683	-0.2836	-0.3235
2.0	5.0	0.3	$\frac{\pi}{4}$	0.2	1.0	2.1323	-0.2850	-0.3233
2.0	5.0	0.4	$\frac{\pi}{4}$	0.2	1.0	1.9470	-0.2857	-0.3232
2.0	5.0	0.5	0	0.2	1.0	1.4918	-0.2879	-0.3228
2.0	5.0	0.5	$\frac{\pi}{8}$	0.2	1.0	1.5794	-0.2875	-0.3229
2.0	5.0	0.5	$\frac{\pi}{6}$	0.2	1.0	1.6459	-0.2871	-0.3230
2.0	5.0	0.5	$\frac{\pi}{4}$	0.2	1.0	1.8290	-0.2862	-0.3231
2.0	5.0	0.5	$\frac{\pi}{4}$	0.2	1.0	1.8290	-0.2862	-0.3231
2.0	5.0	0.5	$\frac{\pi}{4}$	0.4	1.0	1.8695	-0.2911	-0.3220
2.0	5.0	0.5	$\frac{\pi}{4}$	0.6	1.0	1.9523	-0.2965	-0.3209
2.0	5.0	0.5	$\frac{\pi}{4}$	0.8	1.0	2.0692	-0.3013	-0.3199
2.0	5.0	0.5	$\frac{\pi}{4}$	0.2	1.0	1.8290	-0.2862	-0.3231
2.0	5.0	0.5	$\frac{\pi}{4}$	0.2	2.0	1.8261	-0.2324	-0.3287
2.0	5.0	0.5	$\frac{\pi}{4}$	0.2	3.0	1.8241	-0.1970	-0.3324
2.0	5.0	0.5	$\frac{\pi}{4}$	0.2	4.0	1.8226	-0.1766	-0.3351

Table 3: Influence of Du, H, Sr, Kr and Ec on Cf, Nu and Sh.

Du	H	Sr	Kr	Ec	Cf	Nu	Sh
0.5	0.2	1.0	0.5	0.2	1.8263	-0.3338	-0.3274
0.6	0.2	1.0	0.5	0.2	1.8256	-0.3457	-0.3284
0.7	0.2	1.0	0.5	0.2	1.8249	-0.3577	-0.3295
0.8	0.2	1.0	0.5	0.2	1.8242	-0.3696	-0.3306
0.1	0.2	1.0	0.5	0.2	1.8290	-0.2862	-0.3231
0.1	0.4	1.0	0.5	0.2	1.8413	-0.4125	-0.3068
0.1	0.6	1.0	0.5	0.2	1.8428	-0.4935	-0.2865
0.1	0.8	1.0	0.5	0.2	1.8461	-0.5701	-0.2717
0.1	0.2	0.5	0.5	0.2	1.8319	-0.2860	-0.3350
0.1	0.2	1.0	0.5	0.2	1.8290	-0.2862	-0.3231
0.1	0.2	1.5	0.5	0.2	1.8265	-0.2863	-0.3122
0.1	0.2	2.0	0.5	0.2	1.8242	-0.2865	-0.3024
0.1	0.2	1.0	1.0	0.2	1.8541	-0.2879	-0.4807
0.1	0.2	1.0	2.0	0.2	1.8860	-0.2881	-0.7067
0.1	0.2	1.0	3.0	0.2	1.9079	-0.2906	-0.8789
0.1	0.2	1.0	4.0	0.2	1.9249	-0.2933	-1.0231
0.1	0.2	1.0	0.5	0.2	1.8290	-0.2862	-0.3231
0.1	0.2	1.0	0.5	0.4	1.7186	-0.3301	-0.3639
0.1	0.2	1.0	0.5	0.6	1.6123	-0.3768	-0.4244
0.1	0.2	1.0	0.5	0.8	1.5110	-0.4147	-0.4998

APPENDIX

$$
\begin{aligned}
A_1 &= \frac{Pr}{1+R}, \quad A_2 = ScSr, \quad A_3 = \frac{m_1^2}{m_2^2 - m_1^2}, \quad A_4 = A_2A_3, \quad A_5 = 1 - A_4, \\
A_6 &= \frac{(1+NA_4)\cos\alpha}{m_3^2 - m_1^2}, \quad A_7 = \frac{NA_5\cos\alpha}{m_3^2 - m_2^2}, \quad A_8 = \exp(ib\tau) - (A_6 + A_7), \\
A_9 &= \frac{A_1A_5m_2^2}{m_1^2 - m_2^2}, \quad A_{10} = \frac{A_1A_4m_1}{2}, \quad A_{11} = \frac{A_2A_9m_2}{2}, \quad A_{12} = 1 + \frac{2m_1}{m_1^2 - m_2^2}, \\
A_{13} &= \frac{2A_2A_{10}m_1 - A_2A_{10}A_{12}m_1^2 - A_2A_9m_1^2}{m_1^2 - m_2^2}, \quad A_{14} = \frac{(A_9 + NA_{13})\cos\alpha}{m_3^2 - m_2^2}, \\
A_{15} &= \frac{(A_9 + NA_{13})\cos\alpha}{m_3^2 - m_1^2}, \quad A_{16} = 1 + \frac{2m_2}{m_2^2 - m_3^2}, \quad A_{17} = \frac{NA_{11}\cos\alpha}{m_3^2 - m_2^2}, \\
A_{18} &= A_{16}A_{17}, \quad A_{19} = 1 + \frac{2m_1}{m_1^2 - m_3^2}, \quad A_{20} = \frac{A_{10}\cos\alpha}{m_3^2 - m_1^2}, \quad A_{21} = A_{19}A_{20}, \\
A_{22} &= A_{14} + A_{18}, \quad A_{23} = A_{15} + A_{21}, \quad A_{24} = A_{22} - A_{23}, \\
A_{25} &= \frac{A_1A_8^2m_3^2Ec}{4m_3^2 - m_4^2}, \quad A_{26} = \frac{A_1A_6^2m_1^2Ec}{4m_1^2 - m_4^2}, \quad A_{27} = \frac{A_1A_7^2m_2^2Ec}{4m_2^2 - m_4^2}, \\
A_{28} &= \frac{2A_1A_6A_8m_1m_3Ec}{(m_1 + m_3)^2 - m_4^2}, \quad A_{29} = \frac{2A_1A_6A_7m_1m_2Ec}{(m_1 + m_2)^2 - m_4^2}, \\
A_{30} &= \frac{2A_1A_7A_8m_2m_3Ec}{(m_2 + m_3)^2 - m_4^2}, \quad A_{31} = 1 + A_{25} + A_{26} + A_{27} + A_{28} + A_{29} + A_{30}, \\
A_{32} &= \frac{A_2A_{31}m_4^2}{m_4^2 - m_5^2}, \quad A_{33} = \frac{4A_2A_{25}m_3^2}{4m_3^2 - m_5^2}, \quad A_{34} = \frac{4A_2A_{26}m_1^2}{4m_1^2 - m_5^2}, \\
A_{35} &= \frac{4A_2A_{27}m_2^2}{4m_2^2 - m_5^2}, \quad A_{36} = \frac{A_2A_{28}(m_1 + m_3)^2}{(m_1 + 3)^2 - m_5^2}, \quad A_{37} = \frac{A_2A_{29}(m_1 + m_2)^2}{(m_1 + 2)^2 - m_5^2}, \\
A_{38} &= \frac{A_2A_{30}(m_2 + m_3)^2}{(m_2 + 3)^2 - m_5^2}, \quad A_{39} = [1 + A_{32}] - [A_{33} + A_{34} + A_{35} + A_{36} + A_{37} + A_{38}], \\
A_{40} &= \frac{(A_{31} - NA_{32})\cos\alpha}{m_4^2 - m_6^2}, \quad A_{41} = \frac{NA_{39}\cos\alpha}{m_5^2 - m_6^2}, \quad A_{42} = \frac{(A_{25} - NA_{33})\cos\alpha}{4m_3^2 - m_6^2}, \\
A_{43} &= \frac{(A_{26} - NA_{34})\cos\alpha}{4m_1^2 - m_6^2}, \quad A_{44} = \frac{(A_{27} - NA_{35})\cos\alpha}{4m_2^2 - m_6^2}, \quad A_{45} = \frac{(A_{28} - NA_{36})\cos\alpha}{(m_1 + m_3)^2 - m_6^2}, \\
A_{46} &= \frac{(A_{29} - NA_{37})\cos\alpha}{(m_1 + m_2)^2 - m_6^2}, \quad A_{47} = \frac{(A_{30} - NA_{38})\cos\alpha}{(m_1 + m_3)^2 - m_6^2}, \\
A_{48} &= [A_{40} + A_{41}] - [A_{42} + A_{43} + A_{44} + A_{45} + A_{46} + A_{47}],
\end{aligned}
$$

$$
\begin{aligned}
A_{49} &= \frac{A_1A_{39}m_5^2}{m_5^2-m_4^2}, \quad A_{50}=\frac{A_1A_{32}m_4}{2}, \quad A_{51}=\frac{2A_1m_1^2[2A_{34}+A_6A_{23}Ec]}{4m_1^2-m_4^2},\\
A_{52} &= \frac{2A_1m_2^2[2A_{35}-A_7A_{22}Ec]}{4m_2^2-m_4^2}, \quad A_{53}=\frac{2A_1m_3^2[2A_{33}+A_8A_{24}Ec]}{4m_3^2-m_4^2},\\
A_{54} &= \frac{A_1A_{37}(m_1+m_2)^2-2A_1m_1m_2Ec[A_6A_{22}-A_7A_{23}]}{(m_1+m_2)^2-m_4^2},\\
A_{55} &= \frac{A_1A_{38}(m_2+m_3)^2+2A_1m_2m_3Ec[A_7A_{24}-A_8A_{22}]}{(m_2+m_3)^2-m_4^2},\\
A_{56} &= \frac{A_1A_{36}(m_1+m_3)^2+2A_1m_1m_3Ec[A_6A_{24}+A_8A_{23}]}{(m_1+m_3)^2-m_4^2},\\
A_{57} &= A_{49}+A_{51}+A_{52}+A_{53}+A_{54}+A_{55}+A_{56},\\
A_{58} &= 1+\frac{2m_4}{m_4^2-m_5^2}, \quad A_{59}=\frac{A_2m_4[m_4A_{50}A_{58}-m_4A_{57}-2A_{50}]}{m_4^2-m_5^2},\\
A_{60} &= \frac{A_2A_{49}m_5}{2}, \quad A_{61}=\frac{4A_2A_{51}m_1^2}{4m_1^2-m_5^2}, \quad A_{62}=\frac{4A_2A_{52}m_2^2}{4m_2^2-m_5^2},\\
A_{63} &= \frac{4A_2A_{53}m_3^2}{4m_3^2-m_5^2}, \quad A_{64}=\frac{A_2A_{54}(m_1+m_2)^2}{(m_1+m_2)^2-m_5^2}, \quad A_{65}=\frac{A_2A_{55}(m_2+m_3)^2}{(m_2+m_3)^2-m_5^2},\\
A_{66} &= \frac{A_2A_{56}(m_1+m_3)^2}{(m_1+m_3)^2-m_5^2}, \quad A_{67}=-[A_{59}+A_{61}+A_{62}+A_{63}+A_{64}+A_{65}+A_{66}],\\
A_{68} &= 1+\frac{2m_4}{m_4^2-m_6^2}, \quad A_{69}=\frac{[A_{50}A_{68}-A_{57}-NA_{59}]\cos\alpha}{m_4^2-m_6^2}, \quad A_{70}=1+\frac{2m_5}{m_5^2-m_6^2},\\
A_{71} &= \frac{[A_{49}-NA_{67}+NA_{60}A_{70}]\cos\alpha}{m_5^2-m_6^2}, \quad A_{72}=\frac{[A_{51}-NA_{61}]\cos\alpha}{4m_1^2-m_6^2},\\
A_{73} &= \frac{[A_{52}-NA_{62}]\cos\alpha}{4m_2^2-m_6^2}, \quad A_{74}=\frac{[A_{53}-NA_{63}]\cos\alpha}{4m_3^2-m_6^2},\\
A_{75} &= \frac{[A_{54}-NA_{64}]\cos\alpha}{(m_1+m_2)^2-m_6^2}, \quad A_{76}=\frac{[A_{55}-NA_{65}]\cos\alpha}{(m_2+m_3)^2-m_6^2}, \quad A_{77}=\frac{[A_{56}-NA_{66}]\cos\alpha}{(m_1+m_3)^2-m_6^2},\\
A_{78} &= -[A_{69}+A_{71}+A_{72}+A_{73}+A_{74}+A_{75}+A_{76}+A_{77}],\\
m_1 &= \sqrt{HA_1}, \quad m_2=\sqrt{ScKr}, \quad m_3=\sqrt{M+\frac{1}{K}}, \quad m_4=\sqrt{A_1(H+i\omega)},\\
m_5 &= \sqrt{Sc(Kr+i\omega)}, \quad m_6=\sqrt{M+\frac{1}{K}+i\omega}
\end{aligned}
$$

REFERENCES

[1] Q. Li, G. Flamant, X. Yuan, P. Neveu and L. Luo: *Compact heat exchangers: A review and future applications for a new generation of high temperature solar receivers*, Renewable and Sustainable Energy Reviews, **15** (2011), pp. 4855–4875.

[2] M. L. Hunt and C. L. Tien: *Non-darcian flow, heat and mass transfer in catalytic packed-bed reactors*, Chemical Engineering Science, **45** (1990), pp. 55–63.

[3] G. Leccese, D. Bianchi, B. Betti, D. Lentini and F. Nasuti: *Convective and radiative wall heat transfer in liquid rocket thrust chambers*, Journal of Propulsion and Power, **34** (2018), pp. 318–326.

[4] S. M. Khairnasov and A. M. Naumova: *Heat pipes application to solar energy systems*, Applied Solar Energy, **52** (2016), pp. 47–60.

[5] A. Postelnicu: *Influence of a magnetic field on heat and mass transfer by natural convection from vertical surfaces in porous media considering Soret and Dufour effects*, Int. J. Heat Mass Transfer. **47** (2004), pp. 1467–1472.

[6] M. S. Alam, M. Ferdows, M. Ota and M. A. Maleque: *Dufour and Soret effects on steady free convection and mass transfer flow past a semi-infinite vertical porous plate in a porous medium*, Int. J. Appld Mech. Eng. **11** (2006), pp.535–545.

[7] A. A. Afify: *Similarity solution in MHD: Effects of thermal diffusion and diffusion thermo on free convective heat and mass transfer over a stretching surface considering suction or injection*, Comm. Nonlinear Sci. Numer. Simu. **14** (2009), pp. 2202–2214.

[8] M. Venkateswarlu, G. V. Ramana Reddy and D. V. Lakshmi: *Diffusion-thermo effects on MHD flow past an infinite vertical porous plate in the presence of radiation and chemical reaction*, International Journal of Mathematical Archive. **4** (2013), pp. 39–51.

[9] P. O. Olanrewaju and O. D. Makinde: *Effects of thermal diffusion and diffusion thermo on chemically reacting MHD boundary layer flow of heat and mass transfer past a moving vertical plate with suction /injection*, Arab J. Sc. and Eng. **36** (2011), pp. 1607–1619.

[10] O. D. Makinde: *On MHD mixed convection with soret and dufour effects past a vertical plate embedded in a porous medium*, Latin American Applied Research . **41** (2011), pp. 63–68.

[11] M. Venkateswarlu and P. Padma: *Unsteady MHD free convective heat and mass transfer in a boundary layer flow past a vertical permeable plate with thermal radiation and chemical reaction*, Procedia Engineering. **127** (2015), pp. 791–797.

[12] M. Venkateswarlu, G. Upender Reddy and D. Venkata Lakshmi: *Influence of Hall current and heat source on MHD flow of a rotating fluid in a parallel porous plate channel*, J. Korean Soc. Ind. Appl. Math. **22** (2018), pp. 217–239, 2018.

[13] M. Venkateswarlu and D. Venkata Lakshmi: *Dufour and chemical reaction effects on unsteady MHD flow of a viscous fluid in a parallel porous plate channel under the influence of slip condition*, Journal of the Nigerian Mathematical Society. **36** (2017), pp. 369 - 397.

[14] G. S. Seth and S. Sarkar: *Hydromagnetic natural convection flow with induced magnetic field and nth order chemical reaction of a heat absorbing fluid past an impulsively moving vertical plate with ramped temperature*, Bulgarian Chemical Communications. **47** (2015), pp. 66–79.

[15] S. P. Anjali Devi and B. Ganga: *Effects of viscous and joules dissipation on MHD flow, heat and mass transfer past a stretching porous surface embedded in a porous medium*, Nonlinear Analysis: Modelling and Control, **14** (2009), pp. 303–314.

[16] A. Hussanan, M. Z. Salleh, I. Khan, R. M. Tahar and Z. Ismail: *Soret effects on unteady magnetohydrodynamic mixed convection heat and mass transfer flow in a porous medium with Newtonian heating*, MaejoInt. J. Sci. Technol. **9** (2015), pp.224–245.

[17] N. Vedavathi, K. Ramakrishna and K. J. Reddy: *Radiation and mass transfer effects on unsteady MHD convective flow past an infinite vertical plate with Dufour and Soret Effects*, Ain Shams Engineering Journal. **6** (2015), pp. 363–371.

[18] G. S. Seth, B. Kumbhakar and S. Sarkar: *Unsteady hydromagnetic natural convection flow with heat and mass transfer of a thermally radiating and chemically reactive fluid past a vertical plate with Newtonian heating and time dependent free stream*, International Journal of Heat and Technology. **32** (2014), pp. 87–94.

[19] M. Venkateswarlu, G. V. Ramana Reddy and D. V. Lakshmi: *Thermal diffusion and radiation effects on unsteady MHD free convection heat and mass transfer flow past a linearly accelerated vertical porous plate with variable temperature and mass diffusion*, J. Korean Soc. Ind. Appl. Math. **18** (2014), pp. 257 - 268.

[20] M. S. Alam, M. M. Rahman and M. A. Sattar: *MHD free convective heat and mass transfer flow past an inclined surface with heat generation*, Thammasat International Journal of Science and Technology. **11** (2006), pp. 1–8.

[21] R. S. Tripathy, G. C. Dash, S. R. Mishra and S. Baag: *Chemical reaction effect on MHD free convective surface over a moving vertical plate through porous medium*, Alexandria Engineering Journal. **54** (2015), pp.673–679.

[22] M. Venkateswarlu and O. D. Makinde: *Unsteady MHD slip flow with radiative heat and mass transfer over an inclined plate embedded in a porous medium*, Defect and Diffusion Forum, **384** (2018), pp. 31–48.

[23] M. Gnaneswara Reddy, P. Padma and B. Bandari Shankar: *Effects of viscous dissipation and heat source on unsteady MHD flow over a stretching sheet*, Ain Shams Engineering Journal, **6**, (2015), pp.1195–1201.

[24] M. Venkateswarlu, G. V. Ramana Reddy and D. V. Lakshmi: *Effects of chemical reaction and heat generation on MHD boundary layer flow of a moving vertical plate with suction and dissipation*, Engineering International. **1** (2013), pp. 27–38.

[25] V. Malapati and V. L. Dasari: *Soret and chemical reaction effects on the radiative MHD flow from an infinite vertical plate*, J. Korean Soc. Ind. Appl. Math. **21** (2017), pp. 39–61.

[26] E. Magyari and A. Pantokratoras: *Note on the effect of thermal radiation in the linearized Rosseland approximation on the heat transfer characteristics of various boundary layer flows*, Int. Commun. Heat and Mass Transfer. **38** (2011), pp. 554–556.

[27] M. Venkateswarlu, O. D. Makinde and P. Rami Reddy: *Influence of Hall current and thermal diffusion on radiative hydromagnetic flow of a rotating fluid in presence of heat absorption*, Journal of Nanofluids, **8** (2019), pp. 756–766.

[28] N. Siva Kumar, Rushi Kumar and A. G. Vijaya Kumar: *Thermal diffusion and chemical reaction effects on unsteady flow past a vertical porous plate with heat source dependent in slip flow regime*, Journal of Naval Architecture and Marine Engineering. **13** (2016), pp. 51–62.

[29] M . Venkateswarlu, D. Venkata Lakshmi and G. Darmaiah: *Influence of slip condition on radiative MHD flow of a viscous fluid in a parallel porous plate channel in presence of heat absorption and chemical reaction*, J. Korean Soc. Ind. Appl. Math. **20** (2016), pp. 333–354.